Paper

DSP-Based Direct Torque Control (DTC) of Five-Phase Induction Motors

Huangsheng Xu
Student Member, IEEE

Hamid A. Toliyat
Senior Member, IEEE

*Lynn J. Petersen
Member, IEEE

Electric Machines & Power Electronics Laboratory
Department of Electrical Engineering
Texas A&M University
College Station, TX 77843-3128
Phone: (979) 862-3034
Fax: (979) 845-6259
E-mail: toliyat@ee.tamu.edu

*NAVSEA Philadelphia
Machinery Research and Development Directorate
Electrical Systems Department
Philadelphia, PA 19112
Phone: (215) 897-8334
Fax: (215) 897-8380
E-mail: PetersenLJ@nswccd.navy.mil

Abstract

This paper presents a fully digital direct torque control (DTC) scheme for a five-phase induction motor based on a 32-bit floating-point TMS320C32 Digital Signal Processor (DSP). The similarities and differences of DTC of the five-phase and three-phase induction motors are analyzed and investigated. In the case of the five-phase induction motor, DTC method has unique advantages. Compared with 8 voltage vectors of the three-phase induction motor drive system, DTC of the five-phase motor drive system has 32 space voltage vectors with different magnitudes. The increased number of the space voltage vectors enables DTC of the five-phase induction motor greater flexibility in selecting the inverter switching states, and achieves a better control of the stator flux and torque. Simulation and experimental results validate the theoretical analysis, and further demonstrate that DTC of the five-phase induction motor yields better performance than that of the three-phase induction motor.

Key word: Five-phase induction motor, direct toque control

1. Introduction

High phase number drives possess several advantages over the conventional three phase drives such as: reducing the amplitude and increasing the frequency of torque pulsation, reducing the rotor harmonic currents, reducing the voltage per phase, lowering the dc link current harmonics and higher reliability. By increasing the number of phases it is also possible to increase the torque per rms ampere for the same volume machine [1]. When a voltage source inverter is used to supply a motor, its stator harmonic current amplitudes are determined not only by the source amplitude and waveform, but also by the motor leakage inductances at harmonic frequencies. These inductances are a function of the number of phases and can be quite small so that certain harmonic currents have large amplitudes as mentioned by Ward and Harer [2], Abbas et al. [3], and Klingshirn [4]. However, Pavithran et al. [5] have shown that the five-phase drives operate satisfactorily when fed from a pulse width modulation (PWM) inverter.

The high phase order drives are likely to remain limited to specialized applications where high reliability is demanded such as electric/hybrid vehicles, aerospace applications, ship propulsion and high power applications where a combination of several solid states devices form one leg of the drive. Therefore, the requirement of n separate drive units in a multi-phase system is not oppressive for large drives since many of the necessary components are presented in the contemporary designs.

Direct torque control of induction motors, which has been developed in the recent decade, is a powerful control method for motor drives. In principle, the DTC method is based on instantaneous space voltage vector theory. Through the optimal selection of space voltage vectors during each sampling period, direct torque control provides the effective and direct control of the stator flux and torque instead of the current control, a more conventional technique [6], [7]. Thus, the DTC strategy is dependent upon the motor-inverter system, and also, the number of space voltage vectors and the switching frequency directly influence the performance of the DTC system.

It is well known that DTC for the three-phase induction motor drives has eight space voltage vectors, six non-zero active space voltage vectors and two zero space voltage vectors. In order to maintain the stator flux and torque within the limit of two hysteresis bands, DTC of the three-phase motor selects one of the six non-zero space voltage vectors and two zero space voltage vectors during each sampling period. The limited eight space voltage vectors available in DTC of the three-phase induction motor drive system determine the presence of ripple in the stator currents and torque. Several papers [8]-[10] put forward the improvement of the stator currents and torque performance by adopting the double three-phase inverters. These techniques not only require complicated control strategies, but also the employed space vectors [11] are far less than the ideal total number of inverter switch combinations ($2^6 = 64$) because several of the switching combinations overlap. In [12], a PWM strategy for direct self-control of the inverter-fed induction motors by introducing 12 sectors into the stator flux $\alpha - \beta$ trajectory plane and avoiding the use of zero voltage vectors was developed. Although this kind of method offers the reduction of lower order harmonics of the inverter input and output currents, the total harmonic current ripple and the switching frequency are increased. Generally, the objective of these schemes is

to generate more space voltage vectors than those used in the basic DTC control scheme.

In comparison with the three-phase induction motor drives, the five-phase motor drives are supplied with a five-phase voltage source inverter (VSI). In this case, there are two zero voltage states associated with either all of the five upper switches "on" or all of five bottom switches "on". Additionally, there are thirty non-zero modes of the switching. The total number of the five-phase inverter switch combinations is $2^5 = 32$, and thus there are 32 corresponding space voltage vectors. In particular, the 32 space voltage vectors are composed of three sets of the different amplitude vectors, and divide the switching plane into 10 sectors as shown in Fig.1. The ratio of the amplitudes of the voltage vectors is $1:1.618:1.618^2$ from the smallest to the largest vector amplitude, respectively [13]-[16].

Therefore, the five-phase induction motor drives have many more space voltage vectors than the three-phase induction motor drives. The increased number of vectors allows the generation of a more elaborate switching vector table in which the selection of the voltage vectors is made based on the real-time values of the stator flux and torque variations. Moreover, the different amplitudes of the space voltage vectors provide increased flexibility in minimizing the ripple of the stator flux and torque.

In this paper, the proposed DTC scheme is implemented using a 32-bit floating-point TMS320C32 DSP. Operating from a 50 MHz clock, a performance of 25 MIPS, and a peak floating-point performance of 50 MFLOPS executes DTC algorithm with high processing speed and precision. Experimental results for DTC of the five-phase and three-phase induction motor are consistent with the theoretical analysis and simulation results. Significant improvement is achieved in the stator flux and torque of the five-phase induction motor versus the three-phase induction motor.

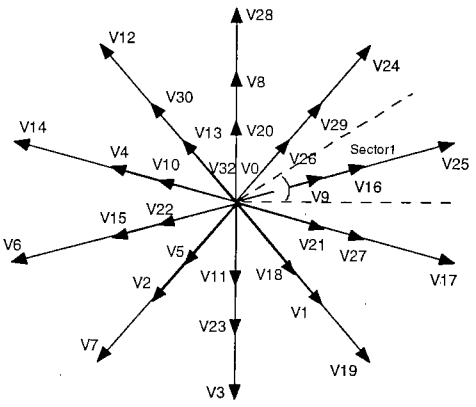

Fig.1 Space voltage vectors of five-phase induction motor.

2. Direct Torque Control Principle of the Five-Phase Induction Motor

A four-pole five-phase induction motor is used for the analysis and test of the developed DTC system. The winding axes of the five stator windings are displaced by $2\pi/5$ *rad.* In order to simplify the analysis, all the stray elements are neglected. The five-phase induction motor is assumed ideal and the iron saturation is also neglected. The basic equations of the five-phase induction motor are expressed in instantaneous vector forms [1], [13]. The voltages V_s and currents I_s for the five-phase induction motor are represented as follows:

$$V_s = \frac{2}{5}[v_a + v_b e^{j\frac{2\pi}{5}} + v_c e^{j\frac{4\pi}{5}} + v_d e^{-j\frac{4\pi}{5}} + v_e e^{-j\frac{2\pi}{5}}] \quad (1)$$

$$I_s = \frac{2}{5}[i_a + i_b e^{j\frac{2\pi}{5}} + i_c e^{j\frac{4\pi}{5}} + i_d e^{-j\frac{4\pi}{5}} + i_e e^{-j\frac{2\pi}{5}}] \quad (2)$$

where v_a, v_b, v_c, v_d, v_e are the instantaneous values of the phase voltages; and i_a, i_b, i_c, i_d, i_e are the instantaneous values of the phase currents. The stationary transformation matrix T is given by:

$$T = \frac{2}{5}\begin{bmatrix} 1 & \cos(\frac{2\pi}{5}) & \cos(\frac{4\pi}{5}) & \cos(\frac{4\pi}{5}) & \cos(\frac{2\pi}{5}) \\ 0 & -\sin(\frac{2\pi}{5}) & -\sin(\frac{4\pi}{5}) & \sin(\frac{4\pi}{5}) & \sin(\frac{2\pi}{5}) \end{bmatrix}$$

Using the five-phase transformation developed in [13] - [15], the dynamic behavior of the five-phase induction motor is described by the following equations written in terms of the space voltage vectors in the stationary reference frame.

Stator and rotor voltages:

$$V_s = R_s I_s + \frac{d\lambda_s}{dt} \quad (3)$$

$$0 = R_r I_r + \frac{d\lambda_r}{dt} - \omega_r J \lambda_r \quad (4)$$

where $J = \begin{bmatrix} 0 & -1 \\ 1 & 0 \end{bmatrix}$.

Stator and rotor flux linkages:

$$\lambda_s = L_s I_s + L_m I_r \quad (5)$$

$$\lambda_r = L_m I_s + L_r I_r \quad (6)$$

$$L_s = \frac{5}{2} L_{ms} + L_{\sigma s} \quad (7)$$

$$L_r = \frac{5}{2} L_{mr} + L_{\sigma r} \quad (8)$$

$$L_m = \frac{5}{2} L_{ms} \quad (9)$$

The electromagnetic torque and mechanical motion equation are expressed by:

$$T_e = \frac{5}{2}\frac{P}{2}(\lambda_s \times I_s) = \frac{5}{2}\frac{P}{2}(I_r \times \lambda_r) \quad (10)$$

$$T_e - T_L = J_m \frac{d\omega_r}{dt} \quad (11)$$

According to (3), the stator flux λ_s can be obtained from:

$$\lambda_s = \int_0^t (V_s - I_s R_s) dt \quad (12)$$

Since the stator resistance R_s is relatively small, the voltage drop $I_s R_s$ might be neglected. The equation above in the discrete time form can be presented as:

$$\lambda_{s(n)} = \lambda_{s(n-1)} + V_s * T \quad (13)$$

where T is the sampling period.

From (12) and (13), it is clear that the stator flux directly depends on the space voltage vector V_s and the sampling period T. Therefore, by properly selecting the thirty-two voltage vectors, V_s, it is possible to control the stator flux, λ_s, and make the stator flux, λ_s move along a predetermined path.

Furthermore, the relationship between the torque of the five-phase induction motor and the space voltage vectors, V_s, is analyzed. From (3) to (9), the following expressions can be derived as in [16]:

$$T_r \frac{d\lambda_r}{dt} = (P\omega_r T_r J - 1)\lambda_r + L_m I_s \tag{14}$$

$$\frac{L_r}{L_m}\lambda_s = \lambda_r + L_\sigma I_s \tag{15}$$

where $T_r = \frac{L_r}{R_r}$; $L_\sigma = \frac{L_s L_r - L_m^2}{L_m}$.

Finally, the torque can be expressed as following:

$$L_\sigma \frac{dT_e}{dt} = P(\lambda_r \times V_s) - R_m T_e - P^2 \omega_r (\lambda_s \cdot \lambda_r) \tag{16}$$

where $R_m = \frac{R_s L_r + R_r L_s}{L_m}$.

In (16), since the stator and rotor flux linkages λ_s, λ_r, and the motor speed ω_r cannot change instantly, only the voltage V_s can be varied with every sampling interval.

According to (5) and (6), the relationship between λ_s and λ_r can be obtained as following:

$$\frac{L_r}{L_m}\lambda_s = \lambda_r + L_\sigma I_s \tag{17}$$

Since L_σ is very small, if $|I_s|$ is limited, the difference between λ_s and λ_r is relatively small, i.e., $\lambda_s \approx \lambda_r$. Hence, (16) can be written as:

$$L_\sigma \frac{dT_e}{dt} \approx P(\lambda_s \times V_s) - R_m T_e - P^2 \omega_r (|\lambda_s|^2) \tag{18}$$

From (18), if holding the stator flux λ_s constant, the proper selection of the space voltage vectors V_s can increase or decrease the torque quickly.

Above all, by employing the different space voltage vectors, V_s, both the stator flux and torque of the five-phase induction motor can be controlled simultaneously.

3. Direct Torque Control Scheme for Five Phase Induction Motor Drives

As described previously, the objective of DTC of the five-phase induction motor is to maintain the stator flux and torque within the limits of the flux and torque hysteresis bands by proper selection of the 32 stator space voltage vectors during each sampling period. The voltage vectors are selected according to the errors of the stator flux and torque ($\Delta\lambda = \lambda^* - \lambda_e$ and $\Delta T = T^* - T_e$). Table 1 summarizes the combined effects of each voltage vector on both the stator flux and torque, assuming the initial stator flux is located in the first sector.

The 32 space voltage vectors are divided into three groups according to their amplitudes. The larger the voltage vector amplitude, the higher its influence is on the flux λ_s and torque T_e. This is illustrated in Table 1 with the number of arrows. Three arrows upward ($\uparrow\uparrow\uparrow$) or downward ($\downarrow\downarrow\downarrow$) represent the maximization or minimization of the flux λ_s and torque T_e when these voltage vectors are applied. The arrow ($\uparrow\downarrow$) indicates that the flux stays nearly constant. The hysteresis bandwidths of the flux and torque related to the three sets of the space voltage vectors are defined by the three different values, 5%, 10% and 15% of the errors of the flux $\Delta\lambda$ and torque ΔT.

When $\Delta\lambda$ and ΔT are within the same band, a single non-zero voltage vector can be selected to satisfy the flux and torque requirements simultaneously. In the proposed DTC schemes, the torque is given priority to have a precise and an effective control. With the combination of the selected voltage vector, V_k $(k = 1...30)$, and zero voltage vectors V_0, V_{32}, the torque error ΔT after one sampling period should be controlled to zero. Obviously, the key is to determine the duration time, T_1, of non-zero voltage vector, V_k, over the sampling period, T_s, and that of zero voltage vectors in the remaining time of $T_s - T_1$. Zero vectors are selected based on minimizing the average switching frequency.

According to (16), T_1 can be obtained as:

$$T_1 = \frac{L_\sigma \Delta T + (R_m T_e + p^2 \omega_r \frac{L_r}{L_m}|\lambda_s|^2)T_s}{p\frac{L_r}{L_m}(\lambda_s \times V_k)} \tag{19}$$

where, $\Delta T = \frac{p(\lambda_r \times V_k) - 2R_m T_e - p^2 \omega_r \lambda_s \cdot \lambda_r}{L_\sigma}$.

In this case, the flux error can be controlled to be very small because of the insertion of zero voltage vectors V_0, or V_{32}.

On the other hand, if $\Delta\lambda$ and ΔT were located in different bands, the two non-zero voltage vectors with different amplitudes should be chosen. The voltage vector with the larger amplitude, V_{k1}, is first adopted to reduce about 5% error of the flux or torque, whose duration time, T_{k1}, can be calculated from (13) or (16), and then the smaller voltage vector, V_{k2}, is employed for the remaining time ($T_{k2} = T_s - T_{k1}$) within one sampling period. Thus, for this case both the flux pulsation and torque pulsation can be minimized.

Because of the 32 space voltage vectors, which can be used for the control of the five-phase induction motor, it is almost impossible to adopt the table-seeking method to complete the selection process for each sampling period in the simulation and the real-time control program. Therefore, a corresponding algorithm, instead of the

conventional table-seeking method, is developed to select the space voltage vectors according to the control scheme described above. This technique greatly reduces the execution time of the real-time control program and shortens the sampling period. Furthermore, it reduces the flux and torque pulsation of the five-phase induction motor.

Table I. Stator Flux and Torque Variations under Different Vectors.

	V_6	V_{14}	V_{12}	V_{28}	V_{24}	V_{25}	V_{17}	V_{19}	V_3	V_7	$V_{0(32)}$
$\lambda_{s(1)}$	↓↓↓	↓↓	↓	↑	↑↑	↑↑↑	↑↑	↑	↓	↓↓	↑↓
$T_{e(1)}$	↓	↑↑	↑↑↑	↑↑↑	↑↑	↓	↓↓	↓↓↓	↓↓↓	↓↓	↓

	V_{15}	V_4	V_{30}	V_8	V_{29}	V_{16}	V_{27}	V_1	V_{23}	V_2	$V_{0(32)}$
$\lambda_{s(2)}$	↓↓↓	↓↓	↓	↑	↑↑	↑↑↑	↑↑	↑	↓	↓↓	↑↓
$T_{e(2)}$	↓	↑↑	↑↑↑	↑↑↑	↑↑	↓	↓↓	↓↓↓	↓↓↓	↓↓	↓

	V_{22}	V_{10}	V_{13}	V_{20}	V_{26}	V_9	V_{21}	V_{18}	V_{11}	V_5	$V_{0(32)}$
$\lambda_{s(3)}$	↓↓↓	↓↓	↓	↑	↑↑	↑↑↑	↑↑	↑	↓	↓↓	↑↓
$T_{e(3)}$	↓	↑↑	↑↑↑	↑↑↑	↑↑	↓	↓↓	↓↓↓	↓↓↓	↓↓	↓

For example, suppose the five-phase induction motor operates in the counter-clockwise direction, which is the positive direction of the speed and torque. At the beginning, the space voltage vector, V_{25}, located within the largest group is applied to start the motor and set up the stator flux within a short time period. Accordingly, the stator flux is defined in the first sector. If the flux, λ_s, is less than the given flux, λ_s^*, one of the voltage vectors, V_{17}, V_{19}, V_{24} and V_{28}, which are the neighbors of V_{25}, and V_{25} itself, can be selected to increase its amplitude. Likewise, the decrement of the flux, λ_s, can be achieved by V_{12}, V_{14}, V_6, V_7 and V_3. What is worth noting is that these vectors affect the stator flux differently; V_{25} and V_6 maximize the flux amplitude, while, V_{17}, V_{24}, V_{14} and V_7 further alter the amplitude, and others minimize the flux amplitude. The zero voltage vectors, V_0 and V_{32}, do not substantially affect the flux, with the exception of the flux weakening due to the voltage drop on the stator resistance. Similar analysis can be applied to the voltage vectors in the second group and the third group. However, the voltage vectors in these two groups do not affect the flux amplitude so significantly like those in the first group. So, they can be utilized for the finer adjustment of the stator flux when the motor runs at the steady state.

Simultaneous control of the stator flux and torque can be achieved according to the following scheme. As shown in Table 1, for the positive speed and the voltage vectors in the first group, the stator flux λ_s and torque T_e is increased by applying either of the two voltage vectors of V_{24} or V_{28}. Likewise, a decrement of the flux λ_s and torque T_e can be obtained by either V_3 or V_7. When the flux λ_s needs to increase whereas the torque T_e needs to decrease, V_{17} or V_{19} could be selected. V_{14} or V_{12} leads to a decrement of the stator flux λ_s and an increment of the torque T_e. Although the zero voltage vectors V_0 and V_{32} almost do not affect the stator flux λ_s significantly, they can be used to decrease the torque T_e. Therefore, when it is required to maintain the stator flux λ_s and decrease the torque T_e, the optimum voltage vector would be V_0 or V_{32}. Similar analysis can be applied to the second and third group of voltage vectors. The selection is carried out for each sampling period in any sector where a proper voltage vector is chosen to minimize the errors of the flux and torque so that the flux λ_s and torque T_e follow the desired values.

For the proposed DTC scheme, the average switching frequency of the five-phase inverter is almost the same as that of the three-phase inverter. In principle, the switching frequency can be up to 10kHz if the sampling period is set at $50\mu s$. Actually, it is difficult for this kind of basic DTC scheme to achieve such a high switching frequency. According to Fig.1 and the description above, when the space voltage vectors change from V_{25} to V_{24}, only one switching device is operated. Correspondingly, the two or three switch statuses are changed from V_{25} to V_{26}, or from V_{16} to V_{29} respectively. Even though the sampling period is very short, only two switching devices within a sector switch on or off. Hence the average switching frequency for DTC of the five-phase induction motor is about $10*2/5=4kHz$. Similarly, for DTC of the three-phase induction motor, only one switching device is mainly operated within a sector. The average switching frequency is approximately $10*1/3=3.3kHz$.

Such a switching frequency is undesirable since the switching capabilities of IGBT are not fully utilized at this voltage level. The low switching frequency for the conventional DTC has been problematic. Some switching frequency regulation methods like the constant torque switching frequency strategy [17], [18] and the variable amplitude control of flux and torque hysteresis bands [11] have been suggested, which reduce the ripples of the currents, flux and torque. In this paper, the basic DTC schemes for the five-phase and three-phase induction motors are applied and compared. The objective is to improve the flux and torque ripples by using increased space voltage vectors for the five-phase induction motor.

4. Implementation Strategy of DTC for Five-Phase Induction Motor

Based on the proposed DTC scheme, a fully digital control system has been implemented. The hardware structure block diagram of this system is represented in Fig.2. It includes the developed five-phase induction motor, the five-phase voltage source inverter (VSI), and a fully

digital controller based on the TMS320C32 DSP, which processes the developed DTC control algorithm, and achieves the desired stator flux and torque control. The fast processing speed of the TMS320C32 allows high sampling rates to be used, and thus establishes the DTC of the five-phase induction motor with higher precision. For the five-phase inverter, IGBTs are used as switching devices. DC link voltage, U_d, the five-phase stator currents i_a to i_e, as well as the motor speed, ω_r, are sampled through A/D converters, which are used to observe the stator flux, λ_s, and torque, T_e, in the real time. Fig. 3 schematically displays the block diagram of the DTC control strategy for the five-phase induction motor. The system includes a cascade of two control loops: the inner torque loop, the flux loop, and the outer speed loop.

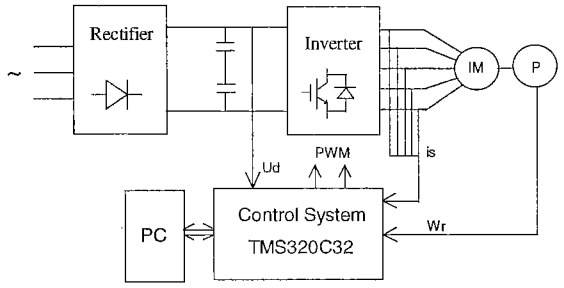

Fig. 2 Experimental setup of DTC for five-phase induction motor.

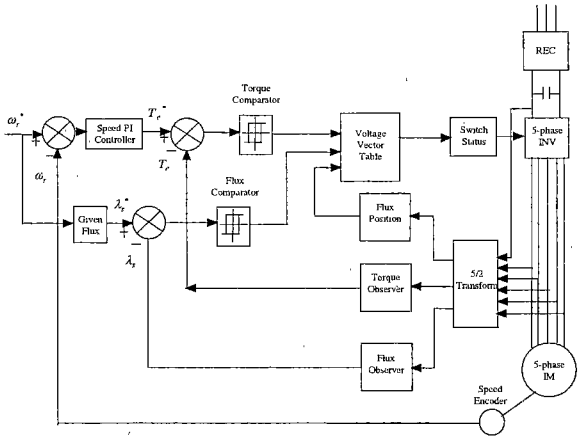

Fig. 3 Block diagram of DTC for five-phase induction motor drive.

Whenever a speed command ω_r^* is given, the system automatically compares it with the motor actual speed ω_r, which is sampled through a speed encoder. According to the motor equation of motion (11), the speed error $\Delta\omega_r$ directly effects the torque profile. Thus, the output of the speed PI regulator can be considered as the torque reference value, T_e^*, to make the necessary torque adjustment. Once the proper adjustment is done, the motor speed should follow the given value, ω_r^*. In the meantime, the five phase stator currents and DC link voltage are sampled to observe the stator flux λ_s and torque, T_e, which are compared with the reference values of the stator flux, λ_s^* and torque, T_e^*. Based on these comparisons, a series of the optimal voltage vectors are generated, which sends out the corresponding switch gating signals to control the five-phase induction motor.

5. Simulation and Experimental Results

The overall five-phase induction motor drive plus the DTC algorithm has been simulated using C language for a 7.5 hp, four-pole, five-phase induction motor, whose parameters are listed in the appendix. The sampling period is equal to $50\mu s$. The reference values are 5Nm for the load torque and 0.5Wb for the stator flux. The motor speed is gradually increased to 300rpm.

In order to verify the improvement of DTC for the five-phase induction motor, a similar simulation also has been performed on a 7.5hp, four-pole, three-phase induction motor with the same sampling frequency and the reference values. Fig. 4 and Fig.5 show the simulation results for the DTC of the five-phase induction motor and the three-phase induction motor.

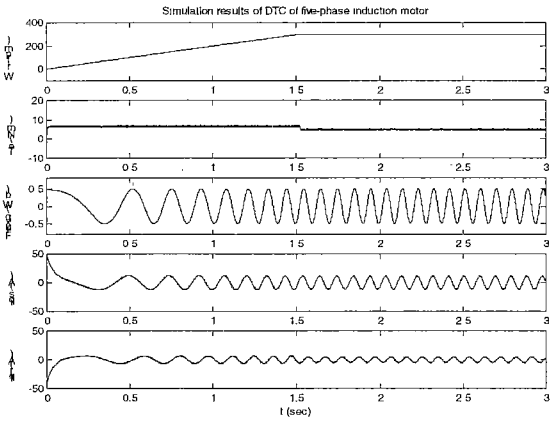

Fig.4 Simulation results for DTC of five-phase inductoin motor, from top to bottom: (a) speed (rpm); (b) torque (Nm); (c) stator q-axis flux (Wb); (d) stator q-axis current I_q (A); (e) rotor q-axis current I_r (A).

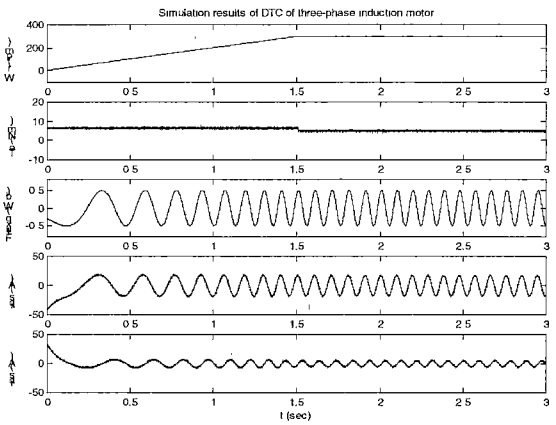

Fig.5 Simulation results for DTC of three-phase inductoin motor, from top to bottom: (a) speed (rpm); (b) torque (Nm); (c) stator q-axis flux (Wb); (d) stator q-axis current I_q (A); (e) rotor q-axis current I_r (A).

It can be seen that fewer ripples for the stator currents and torque is associated with the five-phase induction motor than those with the three-phase induction motor. For the five-phase induction motor, 32 voltage vectors result in a significant improvement of the stator currents and torque, and achieve a more accurate control of them. Because of zero vector application, the flux is controlled more effectively, and thus fluxes for these two cases can perfectly track the commanded value λ_s^* (0.50Wb) with very small ripple.

Experiments have been carried out to compare the performance of DTC for the 7.5hp five-phase induction motor and for the 7.5hp three-phase induction motor by using the TMS320C32 DSP. The sampling period is $50\mu s$, which is approximately the time needed for the execution of the overall control program, including $10\mu s$ for A/D conversion.

Fig.6 through Fig.9 illustrate the experimental results for DTC of the five-phase induction motor and DTC of the three-phase induction motor. The waveforms shown in Fig. 6 and Fig.7 are the stator phase "a" current, i_{sa}, the stator flux, λ_s, and torque, T_e for the DTC of the five-phase induction motor, while Fig. 8 and Fig.9 show the stator phase "a" current, i_{sa}, the stator flux, λ_s and torque, T_e for the DTC of the three-phase induction motor.

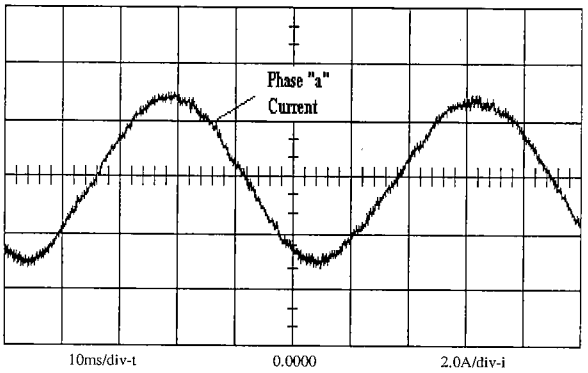

Fig.6 Stator phase "a" current of DTC of five-phase induction motor.

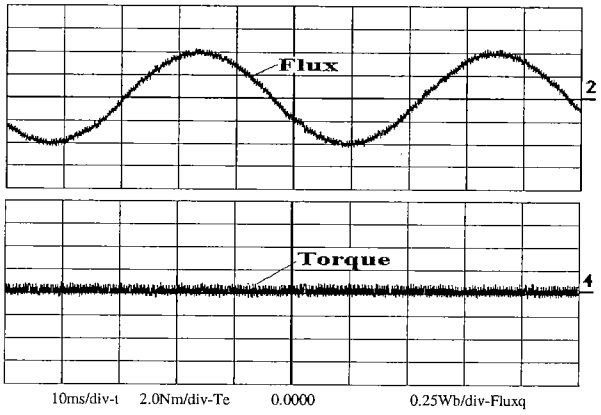

Fig.7 Stator q-axis flux (top) and torque under no load (bottom) for DTC of five-phase induction motor.

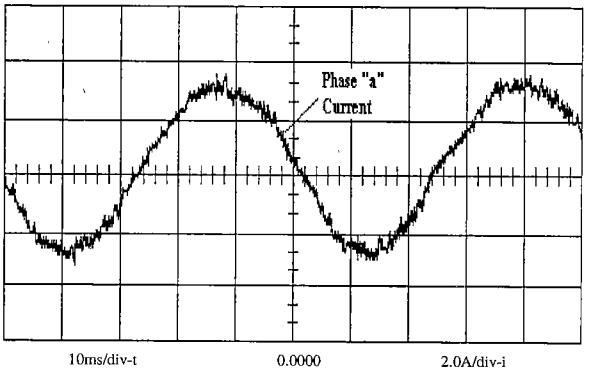

Fig.8 Stator phase "a" current for DTC of three-phase induction motor.

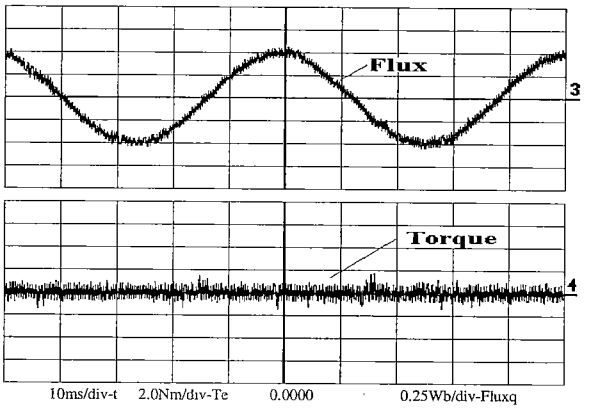

Fig.9 Stator q-axis flux (top) and torque under no load (bottom) for DTC of three-phase induction motor.

By comparing these plots, the performance improvement can be noticed for DTC of the five-phase induction motor from the stator current, the flux and torque ripples, which are obviously less for the five-phase induction motor than those in the three-phase induction motor. These results are consistent with the theoretical analysis and simulation results obtained previously. 32-space voltage vectors for DTC of the five-phase induction motor drives do result in significant reduction of the flux, torque, and the stator current ripples, and implement a more accurate control of the stator flux and the torque.

6. Conclusions

In this paper, a novel DTC method for the five-phase induction motor is presented. The five-phase inverter provides 32 space voltage vectors compared to 8 space voltage vectors for the three-phase inverter. These extra space voltage vectors produce a significant improvement of the torque and current ripples, and achieve a more accurate control of the stator flux and torque for DTC of the five-phase induction motor drive compared with that of the three-phase induction motor drive. For validation and verification purposes, a fully digital DTC control system based on the TMS320C32 DSP for the five-phase induction motor is developed. Both simulation and experimental results demonstrate that a significant improvement is

achieved in the stator currents and torque for DTC of the five-phase induction motor. These results suggest that the combination of DTC with the five-phase induction motor can realize a higher performance. With 32 space voltage vectors offered by the five-phase inverter, several improved control schemes can be further developed for DTC of the five-phase induction motor, such as the application of zero voltage vectors and those voltage vectors with the smaller amplitudes to minimize the ripple in the stator flux and torque.

(Manuscript received Mar. 5, 2001, revised June 15, 2001)

References

[1] H.A. Toliyat, and T.A. Lipo, "Analysis of a Concentrated Winding Induction Motor for Adjustable Speed Drive Applications-Motor Design and Performance", IEEE Transactions on Energy Conversion, Vol. 64, Dec. 1991, pp. 684–692.

[2] E. Ward, and H. Harer, "Preliminary Investigation of an Inverter-Fed 5-Phase Induction Motor", in Proc. Inst. Elect. Eng., vol.116, Jun. 1969, pp. 980-984.

[3] M. Abbas, R. Christen, and T Jahns, "Six-Phase Voltage Source Inverter Driven Induction Motor", IEEE Trans. Ind. Applicat., vol. IA-20, Sep./Oct. 1984, pp. 1251-1259.

[4] E. Klingshirn, "High Phase Order Induction Motors - Part I and II", IEEE Trans. Power App. Sys., vol. PAS-102, Jan 1983, pp. 47-59.T.

[5] K. Pavithran, R. Parimelalagan, and M.R. Krishnamurthy, "Studies on Inverter-Fed Five-Phase Induction Motor Drive", IEEE Trans. Power Electron., vol. 3, Apr. 1988, pp. 224-235.

[6] I. Takahashi, and T. Noguchi, "A New Quick Response and High Efficiency Control Strategy of an Induction Motor", IEEE Trans. Ind. Applicat., vol. IA-22, Sept./Oct. 1986, pp 820-827.

[7] M. Depenbrock, "Direct Self-Control (DSC) of Inverter-Fed IM", IEEE Trans. Power Electron., vol. 3, no. 4, Oct. 1988, pp. 420-429.

[8] I. Takahashi, and Y. Ohmori, "High-Performance Direct Torque Control of an Induction Motor", IEEE Trans. Ind. Applications, vol. 25, Mar./Apr. 1989, pp. 257-264.

[9] Q. Wu and A. Steimel, "Direct Self Control of Induction Machines Fed by a Double Three-level Inverter", IEEE Trans. Ind. Electron., vol. 44, Aug. 1997, pp 519-527

[10] D. Casadei, G. Serra, and A. Tani, " The Use Matrix Converters in Direct Torque Control of Induction Machines", in Proc. IECON'98, vol. 2, 1998, pp 744 –749.

[11] J. Kang, D. Chung, and S. Sul, "Direct Torque Control of Induction Machine with Variable Amplitude Control of Flux and Torque Hysteresis Bands", in Proc. IEMDC '99, 1999, pp. 640 -642.

[12] A. Walczyna, and R. Hill, "Novel PWM Strategy for Direct Self-Control of Inverter-Fed Induction Motors", in Proc. ISIE'93, 1993 , pp. 610 –615.

[13] H. A. Toliyat, M. Rahimian, and T. Lipo, "Analysis and Modeling of Five Phase Converters for Adjustable Speed Drive Applications", in Proc. European Conf. on Power Electronics and Applications, vol. 5, 1993, pp. 194 –199.

[14] H. Toliyat, "Analysis and Simulation of Five-Phase Variable Speed Induction Motor Drives Under Asymmetrical Connections," IEEE Trans. on Power Electron., vol. 13, Jul.1998, pp. 748-756.

[15] H. Toliyat, and H. Xu, "A Novel Direct Torque Control (DTC) Method for Five-Phase Induction Machines", in Proc. APEC'00, vol.1, 2000, pp. 162 -168.

[16] Y. Li, J. Shao, and B. Si, "Direct Torque Control of IM for Low Speed Drives Considering Discrete Effects of Control and Dead-Time of Inverter", in Conf. Rec. IEEE-IAS Annu. Meeting, vol. 1, 1997, pp. 781-788.

[17] N. Idris, and A. Yatim, "Reduced Torque Ripple and Constant Torque Switching Frequency Strategy for Direct Torque Control of Induction Machine", in Proc. APEC'00, vol.1, 2000, pp.154 –161.

[18] J. Kang, S. Sul, "New Direct Torque Control of Induction Motor for Minimum Torque Ripple and Constant Switching Frequency", IEEE Trans. Ind. Applications, vol. 35 5, Sept.-Oct.1999, pp. 1076 –1082.

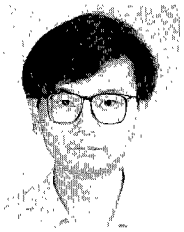

Huangsheng Xu received the B.S. degree in 1989 from Hefei University of Technology, Hefei, China, and the M.S. degree in 1995 from Tsinghua University, Beijing, China, both in electrical engineering. He finished his Ph.D. study at Texas A&M University in September 2001, and currently he is a Senior Engineer at Whirlpool R&E Center, Benton Harbor, Michigan. His research interests include induction motor drives, power electronics and DSP applications.

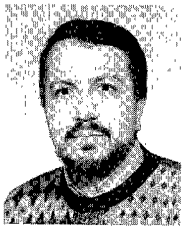

Hamid A. Toliyat received the B.S, degree from Sharif University of Technology, Tehran, Iran in 1982, the M.S. degree from West Virginia University, Morgantown, WV in 1986, and the Ph.D. degree from University of Wisconsin-Madison, Madison, WI in 1991, all in electrical engineering. He is currently an associate professor in the Department of Electrical Engineering, Texas A&M University. He has received the Texas A&M Select Young Investigator Award in 1999, and Eugene Webb Faculty Fellow Award in 2000. He has also received the Space Act Award by NASA in 1999, and the Schlumberger Foundation Technical Award in 2000 and 2001. Dr. Toliyat is an Editor of IEEE Transactions on Energy Conversion, an Associate Editor of IEEE Transactions on Power Electronics, and a member of the Editorial Board of Electric Machines and Power Systems Journal. He is serving on several IEEE committees and subcommittees, and is a member of Sigma Xi. He is the recipient of the 1996 IEEE Power Engineering Society Prize Paper Award. His main research interests and experience include multi-phase variable speed drives for traction and propulsion applications, fault diagnosis of electric machinery, analysis and design of electrical machines, sensorless variable speed drives and has published over 110 technical papers in these fields.

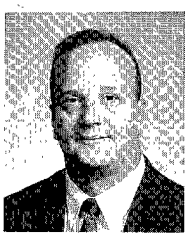

Lynn J. Petersen, is a senior Electrical Engineer within the Machinery Research and Development Directorate of the Naval Surface Warfare Center, Carderock Division (NSWCCD) Philadelphia. He has served as Branch Head for the Electrical Machinery Technology Branch, NSWCCD, and is currently the Deputy Program Manager for the Office of Naval Research "Quiet Electric Drive" Program. He has authored and co-authored numerous papers and reports involving electric machinery for U.S. Naval applications. Mr. Petersen received a Bachelors of Science degree in Mathematics from the United States Naval Academy in 1986 and a Masters of Science degree in Mechanical Engineering from the Naval Postgraduate School in 1994. He has accumulated over 15 years of Naval fleet engineering operational and repair experience having served on two Naval Cruisers and at a naval nuclear shipyard. Additionally, he is an Engineering Duty Officer and a Lieutenant Commander in the Naval Reserve. He is married and has two children